Time-of-flight secondary ion mass spectrometry and X-rayphotoelectron spectroscopy protocol for the analysis oforganic multilaye

Claire Guyot, Jean-Paul Barnes, Olivier Renault, Tony Maindron

▶ **To cite this version:**

Claire Guyot, Jean-Paul Barnes, Olivier Renault, Tony Maindron. Time-of-flight secondary ion mass spectrometry and X-rayphotoelectron spectroscopy protocol for the analysis oforganic multilaye. Surface and Interface Analysis, 2024, 56 (3), pp.129-135. 10.1002/sia.7277 . cea-04475969

HAL Id: cea-04475969

https://cea.hal.science/cea-04475969v1

Submitted on 24 Feb 2024

HAL is a multi-disciplinary open access archive for the deposit and dissemination of scientific research documents, whether they are published or not. The documents may come from teaching and research institutions in France or abroad, or from public or private research centers.

L'archive ouverte pluridisciplinaire **HAL**, est destinée au dépôt et à la diffusion de documents scientifiques de niveau recherche, publiés ou non, émanant des établissements d'enseignement et de recherche français ou étrangers, des laboratoires publics ou privés.

Distributed under a Creative Commons Attribution 4.0 International License

ToF-SIMS and XPS correlative protocol for the analysis of organic multilayers

Claire Guyot[1], Jean-Paul Barnes[1], Olivier Renault[1], Tony Maindron[1]

[1]Univ. Grenoble Alpes, CEA, Leti, F-38000, Grenoble, France

Abstract

With the development in the early 2000s of new cluster ion sputtering sources, a reliable analysis of organic multilayers and interfaces has become possible. Nowadays, ToF-SIMS and XPS depth profiling are routinely used to investigate organic stacks. However, analysis beams can cause bond scission or beam-induced degradations that accumulate in buried layers. We developed a correlative protocol that minimises damages related to analysis beams. It uses a shallow angle bevel crater fabricated inside the ToF-SIMS analysis chamber. With this preparation method, the in-depth information is displayed over the surface of the bevel crater. XPS profiles and high-resolution spectra paired with ToF-SIMS images enable an easy identification of the organic layers and complete understanding of their chemistry. The reduction of beam-induced degradation is achieved by minimising the acquisition times, therefore beam exposure on materials. Finally, an important advantage of this preparation method is that the analysis can be performed on exactly the same spot by multiple techniques. Several ToF-SIMS and XPS acquisitions can be carried out with various parameters (investigation of backscattered Ar_n^+ cluster ion fragments, tandem MS imaging, …) as well as analysis with other techniques that possess limitations in spatial resolution and/or inaptitude to probe buried layers such as Raman or AFM.

Key words: Organic electronic, correlative analysis, ToF-SIMS, XPS, degradation

1. Introduction

When compared to inorganic semiconductors, organic semiconductors offer various specific advantages such as flexibility and transparency of the devices, low material and production costs [1-3]. For the past three decades, these materials have been introduced in different applications: from organic light-emitting diodes (OLEDs) to organic photovoltaics (OPVs) and organic field-effect transistors (OFET). Huge advances in the performances and availability of lab-based characterisation techniques enabled the development and commercialisation of these devices over the last decades. In particular, surface characterisation techniques, such as X-ray- and ultraviolet photoelectron spectroscopy (XPS, UPS) and time-of-flight secondary ion mass spectrometry (ToF-SIMS), provide chemical information that is essential to understand degradation mechanisms and improve the device performances [4-8]. However, because of their surface sensitivity, important information concerning the bulk, buried layers and interfaces are unreachable. To analyse thin film multilayers, a sputter ion gun is therefore necessary.

Monoatomic ion sputtering is inadequate for the analysis of organic layers as the high energy per atom tends to induce a large amount of fragmentation in the bombarded molecules [9]. With the development of new cluster ion sources in the early 2000s [10,11], a reliable analysis of these organic buried layers and interfaces became possible.

Nowadays, it is possible to carry out combined XPS and ToF-SIMS analysis to obtain a full understanding of the chemistry of organic multilayers by depth profiling. However, there are some limitations to conventional depth profiling when analysing organic semiconductors. Indeed, the analysis beams used in XPS and ToF-SIMS may damage organic molecules. High-energy ion bombardment or X-ray exposure can cause bond scission or beam-induced degradation [9,12,13] that accumulate in buried layers when depth profiling. Here, we introduce a correlative protocol to analyse organic semiconductors multilayers in a reproducible and reliable way. This protocol serves to minimise the degradation induced by both analysis beams when investigating buried layers. Furthermore, this approach enables an easy correlation of ToF-SIMS and XPS information as the analysis is performed at the same location of the sample, achieved using a bevel crater where the depth information is displayed over the bevel surface.

2. Bevel crater

In the last decades, different methods to prepare a bevel crater have been investigated. From ultra-low angle microtomy to FIB cross-section or in-situ bevel crater, these methods have demonstrated their ability to provide chemical information when combined with XPS and/or ToF-SIMS [14-18]. However, mechanical methods, ion milling and FIB cross-section damage organic semiconductors and destroy valuable molecular information. The development of argon gas cluster ion beam (Ar-GCIB) in the early 2000s enabled the sputtering of organic semiconductors while preserving molecular information. With an energy shared by every atom forming the cluster, the actual energy per atom is very low (few eV/atom) in comparison with conventional monoatomic sputtering (few keV/atom) [19,20]. Moreover, due to this low energy per atom, the sputtering direction will be mostly oriented horizontally instead of vertically in the case of monoatomic sputtering [9], inducing a lower implantation of the argon atoms inside the organic layers.

Different papers reported the use of an Ar-GCIB to fabricate bevel structures. Mihara et al. demonstrated the combination of monoatomic gun with cluster sputtering to form a bevel crater [21]. First, a mask of damaged organic semiconductors is created with a high-energy monoatomic beam, creating a region where the sputter yield has two orders of magnitude less than pristine organic molecules. The surface is then sputtered with the argon gas cluster ion beam enabling the fabrication of a well-controlled bevel crater as the mask protect underlying material from sputtering. A fine control of the dimension of the crater is achieved but the angle of the bevel crater cannot be modified as the angle of the sputter gun in the analysis chamber is fixed (45°). Another method relies on Zalar rotation while sputtering to form a circularly symmetrical crater, exposing the different layers from the center to the edges of the crater [22]. This approach is easy to implement and available on many instruments. However, it does not provide fine control over the dimensions and angle of the bevel crater, which needs to be extremely small for amplifying ultra-thin buried layers.

A bevel crater with total control over its dimensions and angle can be fabricated varying the fluence of an ion beam over the surface of a sample as demonstrated by Mao *et al.* with a

sputtering of C_{60}^{+} [23]. To fabricate this crater, a FIB-like cross section is operated inside the ToF-SIMS analysis chamber by varying the fluence of the sputtering beam over the surface. Therefore, the in-depth information is converted into a lateral information over the bevel surface (figure 1); hence converting a hundred nanometres thick organic stack into a distance of a few hundred micrometres over its surface. Depending on the dimension of the bevel crater, the grazing angle of the bevel crater (up to 0.005°) can lead to an amplification factor of the organic layers up to 10 000. For instance, a thin layer of 5 nm depth would appear with a dimension of about 50 µm on the bevel surface for a 1000 µm-wide crater. This amplification of the apparent thickness of organic layers enables an easy correlative analysis between ToF-SIMS and XPS, enabling analysis over the same area for both techniques.

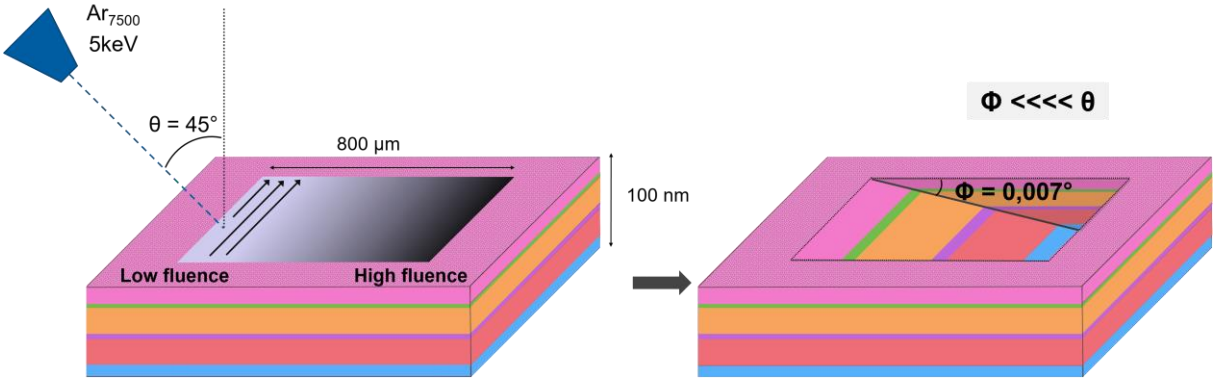

Figure 1. 3D scheme of the bevel crater fabrication process. By applying an increasing ion fluence along the y-direction of the raster area, a bevel-shape crater is formed. Here, an argon-cluster ion beam is used as the sputter gun with an energy of 5 keV and a cluster size of 7500 atoms of argon. In this case, the dimension of the crater is 800 x 800 µm² and the maximum depth is about 100 nm, leading to an angle of 0.007° and an amplification coefficient of the organic layers of about 8700.

3. ToF-SIMS and XPS measurements on organic light-emitting diode multilayer stacks

An example of correlative ToF-SIMS and XPS measurements on a bevel crater is presented on organic light-emitting diode (OLED) multilayers.

The studied green top-emission OLED consists of a five-layer electrically-doped structure sandwiched between an anode of Al : Cu / TiN and a 15 nm-thick silver cathode (figure 2). 1,4,5,8,9,11-Hexaazatriphenylenehexacarbonitrile (HATCN) was used as the 1 nm-thick hole injection layer (HIL). The hole transport layer (HTL) of 30 nm consists of a matrix of 2,2',7,7'-Tetra(N,N-di-p-tolyl)amino-9,9-spirobifluorene (STTB) doped with 4% of 2,3,5,6-Tetrafluoro-7,7,8,8-tetracyanoquinodimethane (F4TCNQ). The electron blocking layer (EBL) consists of 6 nm of N,N′-Bis(naphthalen-1-yl)-N,N′-bis(phenyl)benzidine (NPB). In the emissive layer (EML) of the OLED device, we used 9,9′-(4,4′-(Phenylphosphoryl)bis-(4,1 phenylene))bis(9H-carbazole) (BCPO) as host and tris[2-(p-tolyl)pyridine]iridium(III) ($Ir(mppy)_3$) as triplet dopant, with a doping of 15%. 2,2′,2''-(1,3,5-Benzinetriyl)-tris(1-phenyl-1-H-benzimidazole) (TPBi) is used as the 5 nm-thick hole blocking layer (HBL). Finally, 4,7-Diphenyl-1,10-phenanthroline (BPhen) and Ca were used as host and dopant of the 20 nm-thick electron transport layer (ETL) respectively, with a doping of 4% [24]. The devices are then encapsulated with 80 nm-thick SiO and 25-nm thick Al_2O_3. All organic semiconductors, cathode and SiO

layers were deposited by physical vapor deposition while Al_2O_3 was deposited by low temperature atomic layer deposition [25].

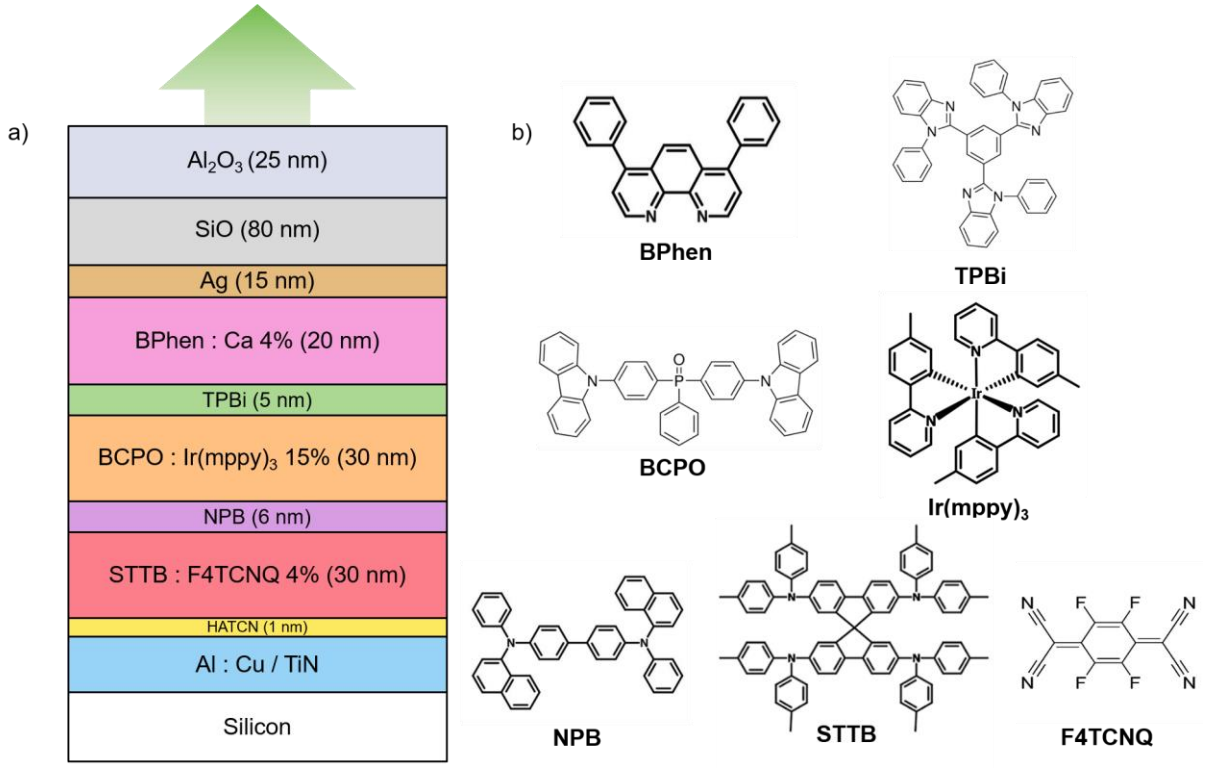

Figure 2. a) Schematic diagram of the device structure and b) utilized organic molecules in this study.

Before introducing the sample mounted on the metallic sample holder with double-sided conductive tape in the ToF-SIMS analysis chamber (TOF-V from IONTOF GmbH), the encapsulation layers and the cathode are peeled off using an adhesive tape under protective atmosphere (N_2)[26]. The bevel crater is then formed in the organic layers using the method described previously. The sputtering is realized with Ar_{7500}^+ ions at an energy of 5 keV with a current around 60 pA. The size of the studied bevel crater is 800 x 800 µm² for a maximum depth of about 100 nm (thickness of the organic stack). As mentioned previously, the layers are extended by the lateral spreading enabled by the bevel crater. Here, the amplification factor is about 8700: for instance, the 5 nm-thick TPBi layer will be converted into a distance of about 43.5 nm on the bevel surface. Finally, the size of the crater has been optimised in order to obtain high intensity with minimum analysis beam exposure (in particular for XPS measurements) as well as fabricating a bevel crater with a controlled raster.

Once the bevel crater is fabricated, ToF-SIMS measurements are first performed as the sample is already present inside the analysis chamber. An image of the surface is acquired with Bi_3^+ primary ions with an energy of 15 keV over an area of 1.1 x 1.1 mm². A wide area is analysed to identify the beginning of the bevel surface. The images were acquired in both polarities with a dose limit of 4.10^{11} ion/cm², ensuring static ToF-SIMS conditions. To each pixel corresponds a mass spectrum, therefore, the identification of the different layers is based on the spatial position of the characteristic molecular ions over the bevel surface as presented in figure 3. a). It is also possible to access to an intensity profile of each characteristic peak (figure 3. b)). To differentiate the bevel surface from the sample surface, common

contamination ions of the surface such as Na^+, K^+ or Cs^+ as well as ions from the diffusion of cathode or encapsulation layer into the organic layers can be used. Here, the surface is identified by the contamination ion Cs^+ remaining in the analysis chamber from previous depth profiling. Its profile confirms that the crater is about 800 µm-long. The exposed distance of the BPhen : Ca layer on the bevel crater is shorter than expected as a non-negligible thickness is removed when the encapsulation layers and the cathode are peeled off [27] .

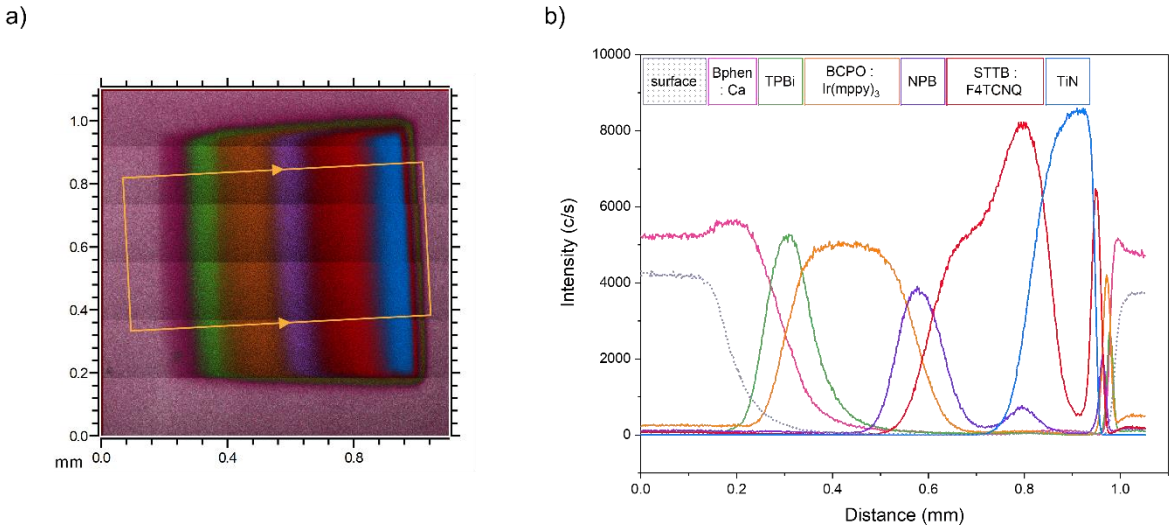

Figure 3. a) Secondary ion image of the surface of the bevel crater and identified layers based on the position of characteristic molecular ions, Ti^+ and Ca^+ ions. The surface is identified by the surface contamination ion Cs^+; b) mean intensity profile of the characteristic molecular ions over the selected area (yellow rectangle).

The sample is then transferred to the XPS analysis chamber (PHI5000 VersaProbe II from Physical Electronics Inc.) under an inert atmosphere (N_2, $P>P_{atm}$) using a transfer vessel. The sample was mounted with double-sided conductive tape onto the metallic sample holder. First, the bevel crater is identified by the difference of image contrast between the organic layers and the substrate on the secondary electron image (figure 4. a)). No chemical contrast amongst the different organic layers is observed as each molecule is mainly composed of carbon and nitrogen. To identify the positions of the layers over the 800 µm-long bevel crater, a profile along a line (linescan) is acquired with a pass energy of 93.3 eV. All XPS measurements are performed using a monochromatized Al Kα source (1486.6 eV) with a beam size of 50 µm and no charge compensation. As the atomic concentration of carbon and nitrogen is very similar in each layer, the organic layers are identified thanks to the profiles of both the characteristic inorganic dopants and substrate. Calcium, iridium and titanium are present in the electron transport layer, emissive layer and the substrate respectively. The positions of the other layers are extrapolated from the dopants and substrate profiles (figure 4. b)). For instance, the TPBi layer, sandwiched between the electron transport layer and the emissive layer, is located at the crossing of the calcium and iridium profiles in the linescan. Afterwards, survey spectra are acquired in each layer. It confirms the correct location of the layers and the elements presents at each position. Finally, high-resolution core-level spectra of and band region spectra are acquired to access the chemical environment of each element. High-resolution spectra and valence band region spectra are acquired with a pass energy of 23.5 eV and 46.95 eV resulting in an overall energy resolution (X-ray bandwidth included) of 0.67 and 0.83 eV respectively.

Valence band region spectra are smoothened using linear Savitzky-Golay smoothing with 5 datapoints. The high-resolution spectra and valence band region spectrum of the emissive layer are presented in figure 4. c). A comparison with reference spectra has been performed on each spectra. However, only the comparison of the valence band region is presented. Indeed, the valence band region of organic compounds acts as a fingerprint [28,29]. Slight chemical modifications may not be observed on core-level spectra but they may be visible in the valence band region. Here, except a shift to lower binding energies (≈ 0.7 eV), the valence band regions are similar regarding the energy separation and relative intensities of its characteristic spectral components. This shift is also observed for all core-level and can be explained by band bending in multilayer structures. Therefore, it is concluded that the fabrication of the bevel crater and the subsequent ToF-SIMS measurements have not induced any detectable damage to the organic molecules.

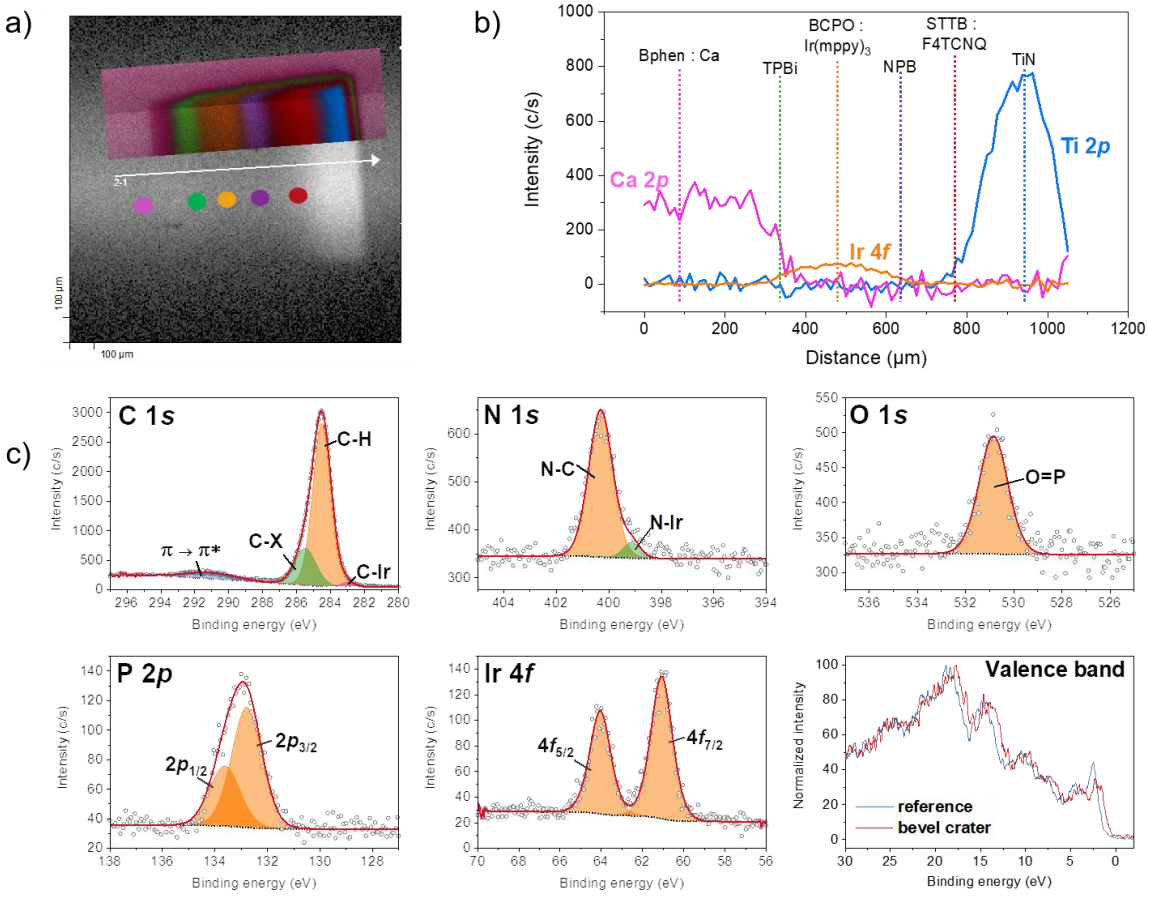

Figure 4. a) secondary electron image of the bevel crater superposed with its complementary image in ToF-SIMS, the XPS linescan (white) and the analysis spot of each layer (coloured dots), b) Ca 2p, Ir 4f and Ti 2p profiles over the surface of the bevel crater along a line and identification of the position of each layer and c) high resolution core-level spectra and valence band region of BCPO : $Ir(mppy)_3$ layer.

4. What are the benefits for the analysis of organic multilayers with this method?

This protocol serves multiple goals. First, the use of a bevel crater provides an easy correlation of ToF-SIMS and XPS results on the same area by locating and individually analysing each layer over the bevel surface, as demonstrated previously.

The second objective concerns the degradations induced by analysis beams. Indeed, modifications of the molecule chemistry and bond scission can occur under illumination and charge neutralization. Here, the described method is not employing any neutralizer whatsoever. In ToF-SIMS, once the Bi_n^{q+} primary ions reach the surface, the cluster will dissociate and penetrate the layers over a distance of about 10-20 nm [30]. The resulting collision cascade into the organic semiconductors can cause bond scission and fragment organic molecules [9]. In XPS, X-ray-induced damages on organic semiconductors have been well documented. Changes in the chemical environment of elements and the ratio of atomic concentration can be observed after an hour of X-ray exposure [12,13]. Moreover, X-rays probe about 9 nm depth into organic semiconductors. As these characterisation techniques are surface sensitive, depth profiling is mandatory to access in-depth information. However, analysis beams induce damages over a depth of about 10 nm, thus buried layers may already be modified before their analysis. With the described preparation method, the in-depth information is displayed over the surface of the bevel without previous analysis beam exposure, preserving the chemical information of buried layers. Furthermore, acquisition times, and therefore analysis beam flux, are reduced in comparison with depth profiling. In ToF-SIMS, images in both polarities are acquired with a primary ion dose of 4.10^{11} ions/cm², ensuring static conditions. In XPS, even though several measurements are performed, the total X-ray exposure time varies from 60 min to 120 min. First, a profile along an 850 µm-length line to identify each layer lasts about 70 min for 85 pixels, resulting in an effective time per pixel of 50 s. Then, survey spectra are acquired in each identified layers for about 3 min. Finally, high-resolution core-level spectra and valence band region are performed for about 50 min to 110 min depending on the number of elements to acquire.

Finally, several measurements can be performed on a bevel crater with different ToF-SIMS and XPS parameters or with other characterisation techniques. Firstly, changing incident energy or primary ion type induces major changes in the ToF-SIMS mass spectrum. With a higher primary ion incident energy, more fragmentation peaks will be present in the mass spectrum. This phenomenon is also observed for smaller cluster or monoatomic primary ions such as Ga^+ and Bi_1^+. Argon cluster Ar_n^+ can also be used as primary ions to probe physical information by studying the backscattering ratio of small argon cluster [31-33]. Tandem MS imaging of the bevel crater can be used to resolve ambiguities [34] or help identify products of degradation [35]. Secondly, the large dimensions and the grazing angle of the crater enables performing other measurements as well, for instance using characterisation techniques with lower spatial resolution such as Raman [36] or techniques with limitations to probe buried layers such as AFM [37].

5. Conclusions

In summary, this paper presents a correlative approach to analyse organic multilayers with minimal beam damage using a bevel crater. Fabricated by varying the fluence of the Ar cluster ions along the y-direction of the raster area over the surface of the sample, the bevel structure exposes the organic layers over its surface. The grazing angle (~0.007°) and the dimensions (800 µm long for a depth of 100 nm) of the bevel crater enable an amplification coefficient of the organic stack of about 8700. An easy correlation is achieved by coupling ToF-SIMS images with XPS profiles and high-resolution spectra. Profiles along the crater provide depth information by locating the organic layers over the bevel surface. The correlation of individual

analysis of organic layers by ToF-SIMS and XPS offers a more complete understanding of the chemistry of organic molecules. A reduction of beam-induced degradation is achieved by minimising the acquisition times, therefore analysis flux. Moreover, compared to depth profiling, the buried layers displayed over the bevel surface have not been previously exposed to analysis beams, ensuring the preservation of their chemical information. Several measurements can be performed on such structure: variation of ToF-SIMS and XPS parameters as well as analysis with other characterisation techniques with limitation in spatial resolution and /or inaptitude to probe buried layers are possible. Finally, this method can be applied to various organic multilayers samples and may be of particular interest for non-homogenous samples such as dye-sensitized solar cells or polymer light-emitting electrochemical cells, where it is critical to analyse the same area of the sample to avoid variations due to sample heterogeneity.

Acknowledgments

This work, carried out on the Platform for NanoCharacterisation (PFNC), was supported by the "Recherches Technologiques de Base" program of the French National Research Agency (ANR).

1. Sekitani T, Someya T. Stretchable, Large-area Organic Electronics. *Advanced Materials.* 2010;22(20):2228-2246.
2. Yin D, Chen Z-Y, Jiang N-R, et al. Highly Flexible Fabric-Based Organic Light-Emitting Devices for Conformal Wearable Displays. *Advanced Materials Technologies.* 2020;5(4):1900942.
3. Abbel R, Galagan Y, Groen P. Roll-to-Roll Fabrication of Solution Processed Electronics. *Advanced Engineering Materials.* 2018;20(8):1701190.
4. Rabelo de Moraes I, Scholz S, Leo K. Influence of the applied charge on the electro-chemical degradation in green phosphorescent organic light emitting diodes. *Organic Electronics.* 2016;38:164-171.
5. Lin WC, Wang WB, Lin YC, et al. Migration of small molecules during the degradation of organic light-emitting diodes. *Organic Electronics.* 2009;10(4):581-586.
6. Wang Q, Williams G, Tsui T, Aziz H. Photochemical deterioration of the organic/metal contacts in organic optoelectronic devices. *Journal of Applied Physics.* 2012;112(6):064502.
7. Nakayama Y, Nguyen TL, Ozawa Y, et al. Complete Demonstration of the Valence Electronic Structure Inside a Practical Organic Solar Cell Probed by Low Energy Photoemission. *Advanced Energy Materials.* 2014;4(7):1301354.
8. Jeon SO, Lee JY. Improved lifetime in organic solar cells using a bilayer cathode of organic interlayer/Al. *Solar Energy Materials and Solar Cells.* 2012;101:160-165.
9. Postawa Z. Sputtering simulations of organic overlayers on metal substrates by monoatomic and clusters projectiles. *Applied Surface Science.* 2004;231-232:22-28.
10. Yamada I, Matsuo J, Toyoda N, Kirkpatrick A. Materials processing by gas cluster ion beams. *Materials Science and Engineering: R: Reports.* 2001;34(6):231-295.
11. Weibel D, Wong S, Lockyer N, Blenkinsopp P, Hill R, Vickerman JC. A C_{60} Primary Ion Beam System for Time of Flight Secondary Ion Mass Spectrometry: Its Development and Secondary Ion Yield Characteristics. *Analytical Chemistry.* 2003;75(7):1754-1764.
12. McLaren RL, Owen GR, Morgan DJ. Analysis induced reduction of a polyelectrolyte. *Results in Surfaces and Interfaces.* 2022;6:100032.
13. Morgan DJ, Uthayasekaran S. Revisiting degradation in the XPS analysis of polymers. *Surface and Interface Analysis.* 2022.
14. Barnes J-P, Djomeni L, Minoret S, et al. Focused ion beam time-of-flight secondary ion mass spectroscopy tomography of through-silicon vias for 3D integration. *Journal of Vacuum Science & Technology B.* 2016;34(3):03H137.
15. Fiducia TAM, Mendis BG, Li K, et al. Understanding the role of selenium in defect passivation for highly efficient selenium-alloyed cadmium telluride solar cells. *Nature Energy.* 2019;4:504-511.
16. Greunz T, Strauß B, Schausberger SE, Heise B, Jachs B, Stifter D. Cryo ultra-low-angle microtomy for XPS-depth profiling of organic coatings. *Analytical and Bioanalytical Chemistry.* 2013;405:7153-7160.
17. Otto S-K, Riegger LM, Fuchs T, et al. In Situ Investigation of Lithium Metal–Solid Electrolyte Anode Interfaces with ToF-SIMS. *Advanced Materials Interfaces.* 2022;9(13):2102387.
18. Iida S-i, Miyayama T, Fisher GL, Hammond JS, Bryan SR, Sanada N. A new approach for determining accurate chemical distributions using in-situ GCIB cross-section imaging. *Surface and Interface Analysis.* 2014;46(S1):83-86.
19. Matsuo J, Ninomiya S, Nakata Y, Ichiki K, Aoki T, Seki T. Size effect in cluster collision on solid surfaces. *Nuclear Instruments and Methods in Physics Research Section B: Beam Interactions with Materials and Atoms.* 2007;257:627-631.

20. Ninomiya S, Ichiki K, Yamada H, et al. Molecular depth profiling of multilayer structures of organic semiconductor materials by secondary ion mass spectrometry with large argon cluster ion beams. *Rapid Commun Mass Spectrom.* 2009;23(20):3264-3268.
21. Mihara I, Havelund R, Gilmore IS. Embedding-Free Method for Preparation of Cross-Sections of Organic Materials for Micro Chemical Analysis Using Gas Cluster Ion Beam Sputtering. *Analytical Chemistry.* 2017;89(9):4781-4785.
22. Yun D-J, Shin Y, Jung CH, et al. Fabrication of Bevel Structures by Means of the Spatial Gradient of Ion Dose in Ar Gas Cluster Ion Beam and Its Unique Characteristics. *Advanced Materials Interfaces.* 2018;5(23):1800825.
23. Mao D, Wucher A, Winograd N. Molecular Depth Profiling with Cluster Secondary Ion Mass Spectrometry and Wedges. *Analytical Chemistry.* 2010;82(1):57-60.
24. Shelhammer D, Cao XA, Liu N, Wang HJ, Zhou YM. Doping effects and stability of calcium in organic electron-transport materials. *Organic Electronics.* 2020;84:105799.
25. Maindron T, Jullien T, André A. Defect analysis in low temperature atomic layer deposited Al2O3 and physical vapor deposited SiO barrier films and combination of both to achieve high quality moisture barriers. *Journal of Vacuum Science & Technology A.* 2016;34:031513.
26. Langer E. *Advanced chemical characterization of organic electronic materials and devices*, Namur; 2019.
27. Shin HJ, Jung MC, Chung J, Kim K, Lee JC, Lee SP. Degradation mechanism of organic light-emitting device investigated by scanning photoelectron microscopy coupled with peel-off technique. *Applied Physics Letters.* 2006;89(6):063503.
28. Drummond IW, Robinson KS, Carrick A, Schmiedel H. Practical polymer film characterisation using high performance XPS methods. *Fresenius' Journal of Analytical Chemistry.* 1993;346(1):200-204.
29. Pireaux JJ, Caudano R. X-ray photoemission study of core-electron relaxation energies and valence-band formation of the linear alkanes. II. Solid-phase measurements. *Physical Review B.* 1977;15(4):2242-2249.
30. Muramoto S, Brison J, Castner DG. Exploring the Surface Sensitivity of TOF-Secondary Ion Mass Spectrometry by Measuring the Implantation and Sampling Depths of Bin and C60 Ions in Organic Films. *Analytical Chemistry.* 2012;84(1):365-372.
31. Mochiji K, Se N, Inui N, Moritani K. Mass spectrometric analysis of the dissociation of argon cluster ions in collision with several kinds of metal. *Rapid Commun Mass Spectrom.* 2014;28(19):2141-2146.
32. Chundak M, Poleunis C, Delmez V, Jonas AM, Delcorte A. Probing the Surface Curie Temperature of Ferroelectric P(VDF-ran-TrFE) Copolymers by Argon Gas Cluster Ion Scattering. *The Journal of Physical Chemistry C.* 2022;126(2):1125-1131.
33. Poleunis C, Cristaudo V, Delcorte A. Temperature Dependence of Arn+ Cluster Backscattering from Polymer Surfaces: a New Method to Determine the Surface Glass Transition Temperature. *Journal of the American Society for Mass Spectrometry.* 2018;29(1):4-7.
34. Fisher GL, Bruinen AL, Ogrinc Potočnik N, et al. A New Method and Mass Spectrometer Design for TOF-SIMS Parallel Imaging MS/MS. *Analytical Chemistry.* 2016;88(12):6433-6440.
35. Iida S-i, Murakami T, Kurosawa Y, Suzuri Y, Fisher GL, Miyayama T. Time-of-flight secondary ion tandem mass spectrometry depth profiling of organic light-emitting diode devices for elucidating the degradation process. *Rapid Commun Mass Spectrom.* 2020;34(7):e8640.

36. Giorgetti E, Margheri G, Delrosso T, Sottini S, Muniz-Miranda M, Innocenti M. A study of the degradation of poly(3-octylthiophene)-based light emitting diodes by Surface Enhanced Raman Scattering. *Applied Physics B.* 2004;79:603-609.
37. Kolosov D, English DS, Bulovic V, Barbara PF, Forrest SR, Thompson ME. Direct observation of structural changes in organic light emitting devices during degradation. *Journal of Applied Physics.* 2001;90(7):3242-3247.